Sol-Gel Synthesis of Dye–Inorganic Hybrid Materials Comprising Silica, Titania and Thiazole Dyes

Ming-Shien Yen*

Department of Materials Engineering, Kun Shan University, Tainan 71003, Taiwan

Abstract *— A series of novel hybrid materials were prepared via the sol-gel process from methyltrimethoxysilane (MTMS) and titanium-n-butoxide (TNB) with heterocyclic thiazole dyes. Heteroaryl 2-aminothiazoles were synthesized on the basis of previous literature, as coupling components that 2-aminothiazoles undergo a coupling reaction with diazonium components p-methoxyaniline in an ice bath to yield heteroaryl thiazole dyes. Sinica/titania/thiazole dye hybrid materials were synthesized via the sol-gel process with a precursor system. Heteroaryl thiazole dyes were also obtained via the hydrolysis-condensation reaction at a constant ratio of vinyltriethoxysilane (VTES), MTMS, and TNB in the presence of a catalyst. The structures of the hybrid materials were characterized using Fourier transform infrared (FTIR) spectroscopy, ^{29}Si-nuclear magnetic resonance (NMR), energy-dispersive X-ray spectroscopy (EDS), and ultraviolet (UV) analysis. According to the experimental results of FTIR, NMR, EDS, and ultraviolet spectra analysis, the MTMS and TNB in the hybrid material could bond thiazole dyes to form the Si–O–Si or Ti–O–Si network structures with a thiazole moiety.*

Keywords — *titania, silica, thiazole dyes, hybrid materials*

I. INTRODUCTION

Organic-inorganic hybrid materials have received increasing interest [1, 2]. They encompass inorganic oxides that function as fillers in organic polymers and solids consisting of polymers or organic molecules in inorganic oxide networks. Organic-inorganic hybrid materials include ceramic materials and polymer materials with multiple complementary functions [3, 4]. The ceramic materials have a very high strength and heat resistance, whereas the polymer materials have good toughness and processing properties. Generally, organic-inorganic hybrid material was fabricated using the sol-gel and intercalation processes. Among them with the sol-gel composite manufacturing approach can suitable for more material of type and process more variability [5].

The sol-gel process is commonly used for preparing inorganic-organic hybrid materials. The interaction between the inorganic and organic components increases while the inorganic phase reaching to nanometer dimension. Hybrid materials have the toughness and working quality because of the organic component, and the rigidity, dimensions and thermal stabilities because of the inorganic component. The inorganic and organic components can integrate to form a homogeneous biphase system via chemical bonding between the organic and inorganic phases [6-10]. Sol-gel processing offers easy manipulation of chemical composition and leads to full usage of precursor materials. Sol-gel processes have been extensively studied and developed since they are well-suited to prepare materials and design devices with specific properties [11, 12]. Sol-gel processes may be divided into two classes depending on the natures of the precursors. The route that involves the use of alkoxide precursors is more versatile. The most important step in this route is the formation of an inorganic polymer via hydrolysis reactions, in which the molecular precursor is transformed into a highly crosslinking solid in a one-pot procedure. Tetra-alkoxysilanes dissolved in organic solvent, such as alcohol, would undergo hydrolysis reaction to form the intermediate sol including silanol functions. Then, the sol, which forms the colloid particles and disperses in the organic solvent, will be dissolved after condensation polymerization. It is important to note that in aqua-organic solvents, the pH value is not well defined. It is merely a measured value and not the exact value of the acidity of the mixture. The resulting gel possessing a cross-linking structure will be sensitive to the pH value in the acidic environment. Under this environment, the hydrolysis rate will be accelerated, and this acceleration will in turn lower the polymerization rate to form a crosslinking network structure and smaller particles. However, alkaline environments will reduce the extent of hydrolysis, resulting in speeding up the polymerization to form a low-uniformity but highly cross-linking network structure. This synthesis method can be used for the preparation of many inorganic materials, including TiO_2, SiO_2, ZrO_2, ZnO, and Al_2O_3 [13-22].

TiO_2 is inexpensive, non-toxic, and biologically, chemically, and photochemically stable. It has high catalytic activity and oxidative capacity, and is thus often added to paints, inks, plastics, paper, fiber,

cosmetics, and food products [23-25]. Silica is a natural material derived from common materials such as quartz, sand, and flint. Silica has a high chemical stability, a low thermal expansion coefficient, and high heat resistance. Mixed oxides of silica/titania can enhance TiO_2 photocatalytic activity and performance [26, 27]. The relatively high thermal stability of the silica phase can be advantageous in some cases [28]. In addition, the readily attainable high surface area of silica can potentially enhance the catalytic activity by making more of the TiO_2 surface readily available to reactants [29]. If the silica and titania phases are sufficiently intermixed in the catalyst, a short traveling distance between the surface-modified silica adsorption sites and the catalytic active sites on the titania phase may result in highly catalytic performance [30, 31].

The molecules of heteroaryl azo dyes contain unshared electron pairs of nitrogen and sulphur, which can easily trigger resonance and cause the π electrons of the compound to leap from the ground state to the excited state. This process facilitates the chromogenic development of the compound [32, 33]. The use of heterocyclic aromatic amines for improving higher tinctorial strength has been well established. 2-Aminothiazole compounds which possess different substituents in the 4-position of analogous derivatives as diazo components tend to bathochromic shifts as compared to analogous dyes derived from benzenoid compounds [34, 35].

In the present study, the sol-gel method is utilized to process mixed oxides of silica/titania with heteroaryl azo dyes in a combined reaction with various ratios of methyltrimethoxysilane (MTMS) and titanium-n-butoxide (TNB) to synthesize multifunctional heteroarylazo dye hybrid materials.

II. EXPERIMENT

A. Analytical Instruments

Fourier transform infrared (FTIR) spectra were recorded on a Bio-Red Digilab FTS-40 spectrometer (KBr). Proton nuclear magnetic resonance (^{1}H-NMR) spectra were obtained on a Bruker Advanced 400-MHz NMR spectrometer, with chemical shifts expressed in δ ppm using tetramethylsilane (TMS) as an internal standard. The ^{29}Si-NMR spectra were collected using a Bruker Advanced 400-MHz NMR spectrometer at 78.49 MHz, with a recycle time of 60 s and 914 scans. Scanning electron microscope (SEM) images were captured using a Philips XL40 field-emission scanning electron microscope. Electronic spectra were recorded using a SHIMADZU UV-1201 from dyes solutions in dimethylformamide (DMF) and ethanol at a concentration of 1×10^{-5} mol L^{-1}.

B. Materials

Vinyltriethoxysilane (VTES), methyltrimethoxysilane (MTMS), *p*-methoxyaniline, titanium-n-butoxide (TNB), and acetophenone were purchased from Acros Co., Ltd., Belgium. Thiourea, sulfuric acid, and iodide were purchased from Hayashi Pure Chemical Ind., Ltd., Japan.

C. Preparation of intermediate 4 and dye 6

4-phenyl-2-amino-thiazole **2** was prepared from a mixture of thiourea, acetophenone, and iodide, as described elsewhere [36]. Yield of crude product 65%; m.p.143-145°C. FTIR (KBr)/cm^{-1}: 3425 (NH), 3110 (C-H); ^{1}H-NMR (DMSO-d_6) δ ppm: 7.07(1H, s, -CH), 7.20 (2 H, s, NH_2), 7.26-7.79 (5 H, m, PhH).

A finely ground powder of p-methoxy-aniline **1** (1.23 g, 0.01 mole) was added to a mixture of 12 mL of hydrochloric and stirred for 20 min. Sodium nitrite (0.72 g, 0.0105 mole) was added in portions to 5 mL of concentrated sulfuric acid at 10°C and stirred for 1 h at 60-65°C. The solution was cooled to below 5°C before the finely ground derivatives were slowly added. The mixture was stirred at 5-10°C until it was clear (1 h). The resulting diazonium solution was used immediately in the coupling reaction. A clear mixed solution of the coupling component 4-phenyl-2-amino-thiazole **2** (2.0 g, 0.01 mole) and 10% sodium carbonate was stirred. The diazonium mixture was added at 0-5°C and the solution was stirred for at least 2 h. This mixture was diluted on its pH raising to 5-6 (by adding aqueous sodium hydroxide or sodium acetate). The solution was then filtered and washed in water to neutralize the pH. The resulting product was filtered, washed with water, and recrystallized from ethanol to give dye **6**. Yield of crude product 50%; m.p. 253-255°C. FTIR (KBr)/cm^{-1}: 3430 (NH), 3105 (C-H), 1179 (O-CH_3); ^{1}H-NMR (DMSO-d_6) δ ppm: 3.80(3H, s, -OCH_3), 7.04(1H, s, -NH_2), 7.40-7.50(5H, m, ArH), 7.61 (2H, d, 3,5-PhH), 7.82 (2H, d, 2,6-PhH).

D. Preparation of precursor 5 and hybrid material 6

Precursor **5** was prepared by mixing dye **4** (3.10 g, 0.01 mole) with VTES (9.5 g, 0.05 mole) in 80 mL of ethanol with stirring at 65 °C for 4 h at pH of 4-5.

Hybrid material **6** was prepared by the condensation of precursor **5** (4.67 g, 0.01 mole), MTMS (1.36g, 0.01 mole), and TNB (3.40 g, 0.01 mole) in 80 mL of ethanol with stirring at 65°C for 4 h, with hydrochloric acid (0.365 g, 0.01 mole) and 5 mL of water added. The hybrid materials $\mathbf{M_1}$-$\mathbf{M_4}$ were prepared using various molar ratios of precursor **5** to MTMS and TNB (1:5:8, 1:10:8, 1:15:8, 1:20:8) in hydrolysis- polycondensation. The hybrid materials $\mathbf{D_1}$-$\mathbf{D_5}$ were prepared using various molar ratios of precursor **5** to MTMS and TNB (1:20:2, 1:20:4, 1:20:6, 1:20:8, 1:20:10) in hydrolysis-polycondensation.

III. RESULTS AND DISCUSSION

A. Synthesis of hybrid material 6

Scheme 1 shows the route used for synthesizing diazo components and heteroaryl monoazo dyes. The

coupling component, using 4-phenyl-2-aminothiazole **2** as the starting materials in the synthesis of the precursor hybrid materials, was obtained by the cyclization of a mixture of thiourea, acetophenone, and iodine. As shown in Scheme 1, a 4-aryl-2-aminothiazoles (coupling component with diazo components p-methoxy aniline) based heteroaryl monoazo dye **3** was prepared. The diazo component p-methoxy aniline was diazotized using sulfuric acid at 0-5°C. Before the end of diazotization, sulphuric acid was added to a diazonium salt solution to remove excess nitrite ions; the diazonium salt solution was then added to an aqueous diluted sodium carbonate solution of coupling component **2**. To complete the coupling reaction, the pH value of the mixture was adjusted from about 5 to 6 by adding 40% sodium hydroxide solution, which promoted the precipitation of the dyes. The presence of acetic acid prevented an abrupt increase in pH [37]. Dye **3** precipitated after the diazonium solution being added; it was then filtered, washed, and air-dried. Then, heteroaryl monoazo dye **6** modified by the addition of VTES **4** at a constant ratio to yield precursor **5**. Finally, hybrid material **6** was prepared via condensation of precursor **5** with MTMS at a constant ratio.

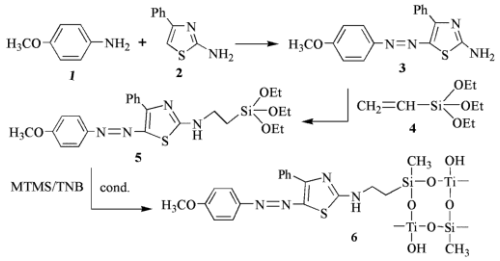

B. FTIR analysis of hybrid materials

The FTIR spectra of the dyes and hybrid materials indicate that dye **3** has N-H, C-H, and O-CH_3 group absorption peaks close to 3430 cm^{-1} and 3105 cm^{-1} and 1179 cm^{-1}, respectively. In the FTIR spectrum of precursor **5**, there is an obvious deviation from the amino group absorption peak, which is close to 3419 cm^{-1}, and the deviated absorption peak is at around 3395 cm^{-1}, revealing that some of the dye had reacted with VTES. The appearance of the Si-OR absorption peak at around 1031 cm^{-1} proves that VTES converted the primary amine group into a secondary amine group, whose absorption peak was at around 3382 cm^{-1}. Therefore, it is reasonable to assume that the reactions between some of the dyes and VTES occurred. The FTIR spectrum of hybrid material **9** includes the absorption peak of the converted secondary amine. The strong capture of the Si-O-Si structure at 1119 cm^{-1} proves the dissociation of the NH_2 bond. The Si-C bond close to 1274 cm^{-1} also reveals that following the dissociation of the NH_2 bond, bonding with CH_2 resulted in linking with Si-O bonds and prompted the formation of the Si-O-Si network. The Ti-O-Ti group and Si-O-Ti group absorption peaks were close to 771 cm^{-1} and 1035 cm^{-1}, respectively. Figures 1 and 2 presenting the FTIR spectra of the hybrid materials $\mathbf{M_1}$-$\mathbf{M_4}$ and $\mathbf{D_1}$-$\mathbf{D_5}$ with various VTES/MTMS/TBT ratios indicate that the increases in the MTMS and TNB concentrations will be accompanied by the increases in the absorption strengths of Si-O-Si close to 1100 cm^{-1}, Ti-O-Ti close to 770 cm^{-1}, and Si-O-Ti close to 1035 cm^{-1}, and strengthens bonding. The structure of Si-O-Si was analyzed using ^{29}Si-NMR.

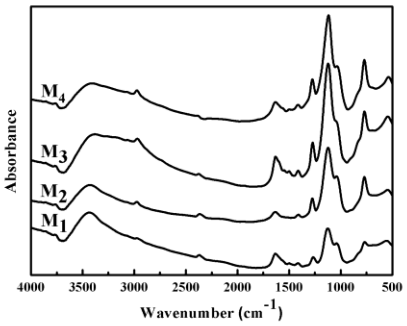

Fig. 1 FT-IR spectra of hybrid materials $\mathbf{M_1}$–$\mathbf{M_4}$

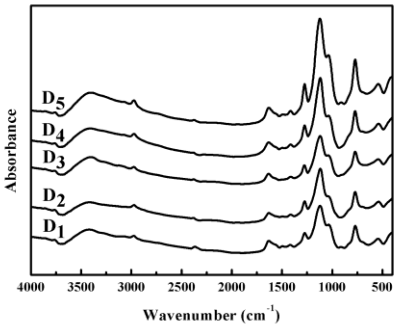

Fig. 2 FT-IR spectra of hybrid materials $\mathbf{D_1}$–$\mathbf{D_5}$

C. Analysis of ^{1}H-NMR and ^{29}Si-NMR

An analysis of the ^{1}H-NMR spectrum of heteroaryl azo dye **3** shows that the benzene ring absorbs the multiplet of dye **3** at δ=7.40-7.50 ppm; the second and sixth positions of the benzene ring absorb the doublet at δ=8.18 ppm; the symmetric hydrogens, 2,6-PhH and 3,5-PhH, absorb the doublet at δ=7.82 ppm and 7.61 ppm, respectively; the singlet at δ=7.04 ppm and 3.80 ppm are absorbed by -NH_2 and -OCH_3, respectively.

^{29}Si-NMR was employed to observe the structure formed by the hydrolysis of Si. While the FTIR results indicate the formation of Si-O-Si by a sol-gel reaction, ^{29}Si solid-state NMR provided data on the structure of silica and the extent of the Si-OH condensation reaction. The high-resolution solid-state NMR spectrum of precursor **5** includes absorption peaks at -65.33 ppm (T^2) and -80.44 ppm (T^3), corresponding to Si-OR following the hydrolysis of VTES. The ^{29}Si-NMR of the hybrid materials $\mathbf{M_1}$-$\mathbf{M_4}$, as shown in Figure 3, indicates that the increase in concentration of MTMS makes the hybrid materials

react more completely, so that the absorption peaks of hybrid materials tend to be smooth. The absorption peak T^3 gradually transforms into the absorption peak Q^1 to form the network structure. Adsorption peak Q^1 is merely changed with the higher MTMS molar ratio that it may be affected by the TNB. The Si-O-Si network structure was little affected when the TNB concentration increased. The formation of Si-O-Ti and Si-O-Si network structures can be generated apparently from the higher molar ratio of MTMS. The ^{29}Si-NMR of the hybrid materials **D_1–D_5**, as shown in Figure 4, illustrates the variation of the absorption peak of T^3 and Q^1 tends to similar with the hybrid materials **M_1-M_4**. The TNB addition increased proportionally, and the network structure of Si-O-Si is merely variation.

D. Analysis of Energy-dispersive X-ray spectra

Table 1 shows the EDS results of the hybrid materials. The molar ratio of a dyes/VTES/MTMS/TNB hybrid material increases with increasing the amount of MTMS, because the $Si(OH)_3$ structure (formed by hydrolysis-condensation of VTES) and SiO_2/TiO_2 (formed after the hydrolysis-polycondensation of MTMS/TNB) would combine with the

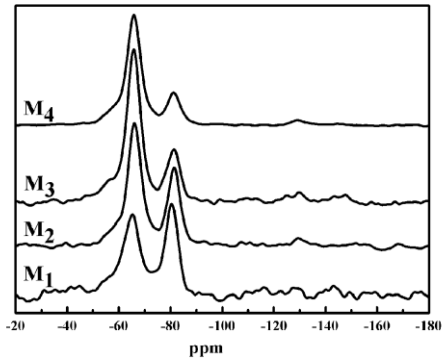

Fig. 3 ^{29}Si-NMR spectra of hybrid material **M_1–M_4**

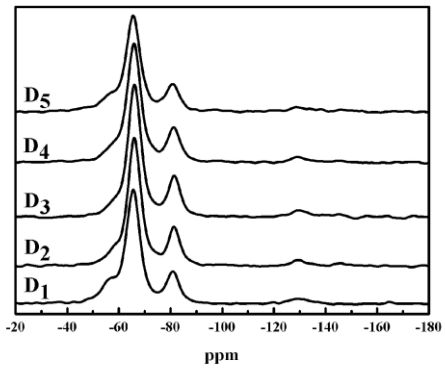

Fig. 4 ^{29}Si-NMR spectra of hybrid materials **D_1–D_5**

dyes. According to Figure 5, the amount of MTMS increased in the hybrid material **M_4**, when the TBT was fixed, the silicon content increased with an increase in the MTMS molar content. According to Figure 6, the amount of TBTNB increased in the hybrid material **D_5**, when the MTMS was fixed, the titania content increased with an increase in the TNB molar content. The Si and Ti peaks revealing a dyes/VTES/ MTMS/TNB hybrid material become more strong intensity as the amounts of MTMS and TNB increase.

Table 1: EDS analysis of hybrid materials **M_1–M and D_1–D_5**

Samples	Elemental composition (%)				
	C	S	O	Si	Ti
M_1	26.77	0.79	24.11	23.35	24.98
M_2	23.83	1.38	26.51	24.45	23.83
M_3	22.60	0.86	26.61	27.70	22.23
M_4	20.50	1.87	26.78	27.98	22.87
D_1	31.62	2.16	23.43	29.81	12.98
D_2	30.82	2.04	23.07	29.15	14.92
D_3	19.92	1.99	25.93	31.45	20.71
D_4	19.90	1.87	26.67	27.98	23.58
D_5	18.11	1.26	26.25	25.45	28.93

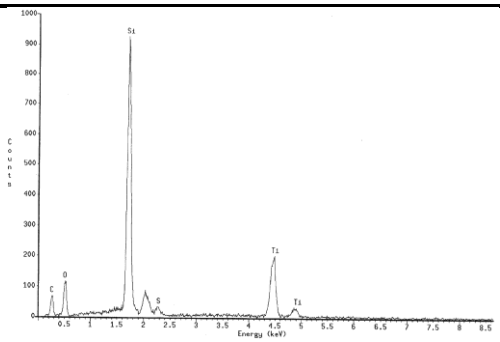

Fig. 5 The EDS diagram of hybrid materials **M_4**

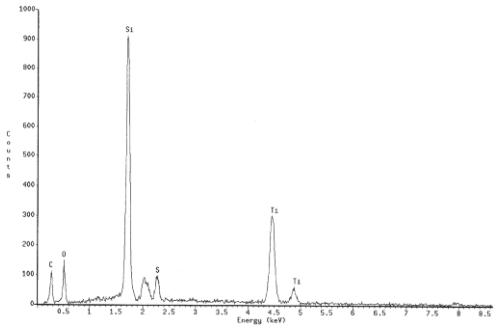

Fig. 6 The EDS diagram of hybrid materials **D_5**

E. Analysis of UV spectra

Table 2 shows the results of the ultraviolet-visible (UV-Vis) absorption spectral analysis of each compound. The results show that increasing MTMS and TNB does not significantly affect λ_{max}. According to the spectra, Figure 7 indicates the hybrid materials **M_4** via the effect of solvents on the compound, dissolution in DMF increases λ_{max}. Since the dipole moment of ethanol is smaller than that of

DMF and a greater dipole moment induces resonance among molecules more easily, less energy is required for dissolution in DMF than in ethanol; consequently, the absorption wavelength is higher.

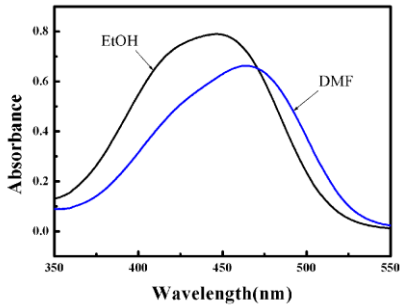

Fig. 7 UV spectra of hybrid material $\mathbf{M_4}$ in various solvents.

IV. CONCLUSIONS

In this study, we synthesized a series of heteroaryl thiazole azo dyes, and then added MTMS/TBT in different ratios to prepare a series of hybrid materials using the sol-gel method. The Si–O–Ti absorption peaks were observed from the FT-IR characterizations, and the intensities of these absorption peaks increased with increasing MTMS amount. On ^{29}Si-NMR determinations the hybrid gels, including $\mathbf{M_4}$ and $\mathbf{D_5}$, showed the absorption peak T^3 gradually transforms into the absorption peak Q^1 at the maximum ratio, suggesting the occurrences of Si–O–Ti and Si–O–Si networks. The ultraviolet spectra analysis showed that different solvents caused differences, and λ_{max} is greater for DMF than ethanol. According to the experimental FTIR, NMR, and energy-dispersive X-ray spectroscopy results, the titania/silica in the hybrid material could bond thiazole azo dyes to form the Si–O–Ti or Si–O–Si network structures with a thiazole moiety.

ACKNOWLEDGMENT

The authors thank the Ministry of Science and Technology of the Republic of China, Taiwan, for financially supporting this research under grant NSC-100-2622-E- 168- 001-CC3.

REFERENCES

[1] J. D. Mackenzie, "Structures and properties of ormosils," *J. Sol-Gel Sci. Technol.*, vol. 2(1-3), pp. 81–86, 1994.

[2] D. A. Loy and K. J. Shea, "Bridged polysilsesquioxanes highly porous hybrid organic- inorganic materials," *Chem. Rev.*, vol. 95(5), pp. 1431–1442, 1995.

[3] B. Ou and D. Li, "The Effect of Functionalized-TiO_2 on the Mechanical Properties of PP/PA6/Functionalized-TiO_2 Nanocomposites Prepared by Reactive Compatibilization Technology," *J. Compos. Mater.*, vol. 43, pp. 1361–1372, 2009.

[4] T. Jeong et al., "3-Aminopropyltriethoxysilane Effect on Thermal and Mechanical Properties of Multi-walled Carbon Nanotubes Reinforced Epoxy Composites," *J. Compos. Mater.*, vol. 43, pp. 2533–2541, 2009.

[5] S. Vives and C. Meunier, "Mixed SiO_2-TiO_2 (1:1) sol-gel films on mild steel substrates: Sol composition and thermal treatment effects," *Surf. Coat. Technol.*, vol. 202, pp. 2374–2378, 2008.

[6] P. Judeinstein and C. Sanchez, "Hybrid organic-inorganic materials: A land of multidisciplinary," *J. Mater. Sci.*, vol. 6 (4), pp. 511–525, 1996.

[7] J. A. Wen and J. E. Mark, "Synthesis, structure, and properties of poly(dimethylsiloxane) networks reinforced by in situ-precipitated silica-titania, silica-zirconia, and silica-alumina mixed oxides," *J. Appl. Polym. Sci.*, vol. 58(7), pp. 1135–1145, 1995.

[8] L. Matejka, O. Dukh and J. Kolarik, "Reinforcement of crosslinked rubbery epoxies by in-situ formed silica," *Polymer*, vol. 41(4), pp. 1449–1459, 2000.

[9] W. Zhou, J. E. Mark, M. R. Unroe and F. E. Arnold, "Toughening of a high-temperature polymer by the sol-gel in situ generation of a rubbery silica-siloxane phase," *J. Appl. Polym. Sci.*, vol. 79(13), pp. 2326–2330, 2001.

[10] C. L. Jackson, B. J. Bauer and A. I. Nakatani, "Synthesis of hybrid organic-inorganic materials from interpenetrating polymer network chemistry," *Chem. Mater.*, vol. 8(3), pp. 727–733, (1996).

[11] L. L. Hench and J. K. West, "The sol-gel process," *Chem. Rev.*, vol. 90, pp.33–72, 1990.

[12] C. D. Chandler, C. Roger and M. J. Hampden-Smith, "Chemical aspects of solution routes to perovskite-phase mixed-metal oxides from metal-organic precursors," *Chem. Rev.*, vol. 93, pp. 1205–1241, 1993.

[13] M. Houmard et al., "Morphology and natural wettability properties of sol-gel derived TiO_2-SiO_2 composite thin films," *Appl. Sur. Sci.*, vol. 254, pp. 1405–1414, 2007.

[14] Z. Jiwei, Y. Taob, Z. Liangying and Y. Xia, "The optical waveguiding properties of TiO_2-SiO_2 composite films prepared by the sol-gel process," *Ceram. Int.*, vol. 25, pp. 667–670, 1999.

[15] H. You and M. Nogami, "Persistent spectral hole burning of Eu^{3+} ions in TiO_2-SiO_2 glass prepared by sol-gel method," *J. Alloys Compd*., vol. 408-412, pp. 796–799, 2006.

[16] H. J. Hah and S. M. Koo, "Surface modification of PTMS particles with organosilanes: TEOS-, VTMS-, and MTMS-modified particles," *J. Sol-Gel Sci. Technol.*, vol. 31, pp. 117–121, 2004.

[17] D. S.Hinczewski, M. Hinczewski, F. Z. and G. G. Tepehan, "Optical filters from SiO_2 and TiO_2 multi-layers using sol-gel spin coating method," *Sol. Energ. Mater. Sol. C.*, vol. 87, pp. 181–196, 2005.

[18] J. Castaneda-Contreras, M. A. Meneses-Nava, O. Barbosa-Garcıa, J. L. Maldonado-Rivera and J. F. Mosino, "Dependence of Er^{3+} blue up-conversion on TiO_2 contents in SiO_2-TiO_2 sol–gel powder," *Optic. Mater.*, vol. 27, pp. 301–305, 2004.

[19] B. Tyagi, K. B. Sidhpuria, B. Shaik and R. V. Jasra, "Effect of Zr-Si molar ratio and sulfation on structural and catalytic properties of ZrO_2-SiO_2 mixed oxides," *J. Porous Mater.*, vol. 17, pp. 699–709, 2010.

[20] R. Linacero, M. L. Rojas-Cervantes and J. D. D. Lopez-Gonzalez, "Preparation of $xTiO_2{\cdot}(1\text{-}x)Al_2O_3$ catalytic supports by the sol-gel method: physical and structural characterization," *J. Mater. Sci.*, vol. 35, pp. 3279–3287, 2000.

[21] S. Sivakumar, C. P. Sibu, P. Mukundan, P. K. Pillai and K. G. K. Warrier, "Nanoporous titania-alumina mixed oxides an alkoxide free sol-gel synthesis," *Mater. Lett.*, vol. 58, pp. 2664–2669, 2004.

[22] C. Shifu, Z. Wei, L. Wei and Z. Sujuan, "Preparation, characterization and activity evaluation of p-n junction photocatalyst p-NiO/n-ZnO," *J. Sol-Gel Sci. Technol.*, vol. 50(3), pp. 387–396, 2009.

[23] S .A. Amin, M. Pazouki and A. Hosseinnia, "Synthesis of TiO_2-Ag nanocomposite with sol–gel method and investigation of its antibacterial activity against," *Powder Technol.*, vol. 196, pp. 241–245, 2009.

[24] M. Houmard et al., "Enhanced persistence of natural super-hydrophilicity in TiO_2-SiO_2 composite thin films deposited via a sol–gel route," *Surf. Sci.*, vol. 602, pp. 3364–3374, 2008.

[25] S. Ivanovici and G. Kickelbick, "Synthesis of hybrid polysiloxane-MO_2 (M = Si, Ti, Zr) nanoparticles through a sol–gel route," *J. Sol-Gel Sci. Technol.*, vol. 46, pp. 273–280, 2008.

[26] O. Kesmez, H. E. Camurlu, E. Burunkaya and E. Arpac, "Sol–gel preparation and characterization of anti-reflective and self-cleaning SiO_2-TiO_2 double-layer nanometric films," *Sol. Energ. Mater. Sol. C.*, vol. 93, pp. 1833–1839, 2009.

[27] R. M. Mohamed and I. A. Mkhalid, "The effect of rare earth dopants on the structure. surface texture and photocatalytic properties of TiO_2-SiO_2 prepared by sol-gel method," *J. Alloys Compd*., vol. 501, pp. 143–147, 2010.

[28] C. Anderson and A. J. Bard "An improved photocatalyst of TiO_2/SiO_2 prepared by a sol–gel synthesis," *J. Phys. Chem.*, vol. 99, pp. 9882–9885, 1995.

[29] C. Anderson and A. J. Bard, "Improved photocatalytic activity and characterization of mixed TiO_2/SiO_2 and TiO_2/Al_2O_3 materials," *J. Phys. Chem. B*, vol. 101, pp. 2611–2616, 1997.

[30] X. Fu, L. A. Clark, Q. Xang and M. A. Anderson, "Enhanced photocatalytic performance of titania based binary metal oxides: TiO_2/SiO_2 and TiO_2/ZrO_2," *Environ. Sci. Technol.*, vol. 30, pp. 647–653, 1996.

[31] Y. Li and S. J. Kim, "Synthesis and characterization of nano titania particles embedded in mesoporous silica with both high photocatalytic activity and adsorption capability," *J. Phys. Chem. B*, vol. 109(25), pp. 12309–12315, 2005.

[32] I. Zadrozna and E. Kaczorowska, "Synthesis and characteristics of azo chromophores for nonlinear-optical application," *Dyes Pigm.*, vol. 71, pp. 207–211, 2006.

[33] M. S. Yen and I. J. Wang, "Synthesis and absorption spectra of hetarylazo dyes derived from coupler 4-aryl-3-cyano-2-aminothiophenes," *Dyes Pigm.*, vol. 61, pp. 243–250, 2004.

[34] A.T. Peters and S. S. Yang, "Monoazo disperse dyes derived from nitro-2-aminobenzothiazoles, Dyes and Pigments, vol. 28, pp. 151–164, 1995.

[35] G. Hallas and J. H. Choi, "Synthesis and spectral properties of azo dyes derived from 2-aminothiophenes and 2-aminothiazoles," *Dyes Pigm.*, vol. 42, pp. 249–265, 1999.

[36] S. N. Pandeya, D. Sriram, G. Nath and E. DeClercq, "Synthesis, antibacterial, antifungal and anti-HIV activities of Schiff and Mannich bases derived from isatin derivatives and N-[4-(4′-chlorophenyl)thiazol-2-yl] thiosemicarbazide," *Eur. J. Pharm. Sci.*, vol. 9, pp. 25–31, 1999.

[37] M. S. Yen and I. J. Wang, "A facile syntheses and absorption characteristics of some monoazo dyes in bis-heterocyclic aromatic systems Part II:Syntheses of 4-(p-substituted) phenyl-2-(2-pyrido-5-yl and 5-pyrazolo-4-yl) azothiazole derivatives," *Dyes Pigm.*, vol. 63, pp. 1–9, 2004.